Frequency-dependent transport properties in disordered systems: A generalized coherent potential approximation approach

Lei Zhang,[1,4] Bin Fu,[2] Bin Wang,[3] Yadong Wei,[3] and Jian Wang[2,*]

[1]*State Key Laboratory of Quantum Optics and Quantum Optics Devices, Institute of Laser Spectroscopy, Shanxi University, Taiyuan 030006, China*

[2]*Department of Physics and the Center of Theoretical and Computational Physics, The University of Hong Kong, Pokfulam Road, Hong Kong, China*

[3]*College of Physics and Energy, Shenzhen University, Shenzhen 518060, China*

[4]*Collaborative Innovation Center of Extreme Optics, Shanxi University, Taiyuan 030006, China*

(Received 12 November 2018; revised manuscript received 28 February 2019; published 5 April 2019)

To predict transport properties of disordered systems, especially ac transport properties, one has to calculate the disorder average of the correlation of the multiple Green's function at different energies. To avoid brute force calculation, diagrammatic perturbation expansion must be used along with the coherent potential approximation (CPA). In this paper, we develop a theoretical formalism based on the nonequilibrium Green's function that maps the average of the correlation of the multiple Green's function into an average over a single generalized Green's function. After the mapping, this formalism is structurally very similar to the CPA and completely eliminates the need to perform diagrammatic expansion. As a demonstration of our theory, the dynamic conductance, frequency-dependent shot noise under dc bias, and frequency-dependent noise spectrum under ac bias in the presence of Anderson disorder are calculated by directly taking the disorder average of the generating function of full counting statistics (FCS) within the CPA. Our numerical results on dynamic conductance, frequency-dependent shot noise under dc bias, and frequency-dependent noise spectrum under ac bias show remarkable agreement with that obtained by the brute force calculation. The phase diagram in the frequency versus disorder strength plane has been efficiently calculated using the generalized FCS-CPA method.

DOI: 10.1103/PhysRevB.99.155406

I. INTRODUCTION

Recently, the frequency-dependent transport properties of mesoscopic and nanoscale systems have attracted intense research attention on both the experimental and theoretical sides [1–23] since they can provide unique insight into the dynamic information of the system. So far, a variety of frequency-dependent quantities, including frequency-dependent shot noise [3,8,11,18], ac conductance [16], frequency-dependent quantum capacitance [15], and time-dependent transient current [5] and charge relaxation resistance [13], has been studied. For example, the dynamic conductance $G_{\alpha\beta}$ has been used to probe the charge and potential distribution in the system [2]. In the quantum capacitor, it was found that the frequency-dependent electrochemical capacitance $C(\omega)$ is equivalent to a classical *RLC* circuit characterized by three quantum parameters, i.e., quantum resistance [14], capacitance [1], and inductance. In the high-frequency regime, the quantum inductance dominates and characterizes the timescale of electron dynamics in the system [15]. When the electron-electron interaction is included, the Kondo resonance in the quantum dot can be extracted from the ac transport conductance and frequency-dependent shot noise [18].

It is known that impurities play an important role in modifying the electronic transport properties of the nanoscale system. On the one hand, people intentionally introduce foreign atoms into the semiconductor that can control its electric or optical properties, which is essential in the development of the current semiconductor industry [24]. On the other hand, the random impurities, defects, and roughness inevitably emerge during the fabrication of materials and devices, which may cause performance degradation. Thus, the disorder effect has always been important throughout the material growth and device fabrication process. In the theoretical condensed-matter physics community, the disorder effect in the mesoscopic system is a fundamentally important issue [25–29]. As one of the hallmarks of mesoscopic physics, the universal charge or spin-Hall conductance fluctuation appears in the diffusive regime when Anderson disorder is present in the system [30–36].

While the disorder effect of dc transport properties such as conductance has been well studied, the role of disorder in frequency-dependent transport properties has received less attention. It is our intention to fill this gap. In order to treat the disorder effect, people have developed theoretical approaches such as the random matrix theory (RMT) for dc [37] and ac transport [38] and the scattering matrix theory (SMT) [39]. Using these approaches, general physics such as the universal conductance fluctuation can be discussed using RMT or SMT in the diffusive regime. In order to have quantitative information about disordered systems, a numerical calculation has to be performed. Numerical brute force calculations taking several thousand or even 100 000 configurations are

*jianwang@hku.hk

frequently used to study average transport properties using either non-equilibrium Green's function (NEGF) or SMT [27,29]. The brute force method is accurate but extremely time-consuming and is sometimes unsuitable for a finite system with a low doping concentration. In view of this limitation, people have developed various approximate methods to formulate the average transport quantities analytically to avoid sampling over different random configurations. Since most transport properties are related to the Green's function, the coherent potential approximation (CPA) method is the state-of-the-art method aiming to calculate the average of a single Green's function. Within the CPA, dc conductance and the nth-order cumulant of dc conductance have been studied using diagrammatic perturbation expansion [11,40–53]. Based on these approaches, ac dynamic conductance has been studied in a one-dimensional toy model via the diagrammatic approach to calculate Green's function correlators [52]. Since diagrammatic expansions for ac conductance are extremely complicated and difficult to implement in the numerical calculations, a simpler and systematic way of calculating frequency transport properties in disordered system needs to be developed. Recently, combining full counting statistics (FCS) [54–57] with the CPA, a simple, effective FCS-CPA theory was developed by us to study the nth-order cumulant of disordered dc conductance [58]. We note that in this theory, all the Green's functions involved have the same energy. To deal with frequency-dependent transport, one must study the disordered average of the multiple Green's function at different energies. Clearly, there is a need to generalize the existing FCS-CPA designed for dc transport to the ac case. In this work, we extend this formula to the frequency-dependent case and develop a theoretical formula to account for the frequency-dependent transport properties of disordered systems. Three examples are given to illustrate the idea of our formalism. Specifically, we have calculated the averaged ac conductance, the frequency-dependent shot noise under dc bias, and the frequency-dependent noise spectrum under ac bias on a two-dimensional square lattice in the presence of Anderson disorders. Remarkable agreement between the brute force calculation and FCS-CPA is demonstrated numerically.

This paper is organized as follows. In Sec. II, we introduce the theoretical formalism for calculating the generating function of the FCS needed to calculate the average frequency-dependent transport properties. As an example, we will apply our method to the tight-binding square-lattice system and will show the numerical results in Sec. III. Finally, Sec. IV contains our discussion and conclusion.

II. THEORETICAL FORMALISM

In order to generalize the FCS-CPA approach from the dc case to calculate frequency-dependent quantities in the presence of disorder, we have to first design a cumulant generating function (CGF) so that the desired quantities can be obtained by taking the derivative of the CGF with respect to the counting field parameter λ in the clean system. Then combining the CGF with the CPA, one can calculate the disorder-averaged quantities from the disorder-averaged CGF. In this section, we illustrate our method of calculating frequency-dependent transport properties within the CPA method using three examples: (1) dynamic conductance of disordered systems, (2) frequency-dependent shot noise under dc bias in the presence of disorders, and (3) the frequency-dependent noise spectrum under ac bias in the presence of disorders.

A. Dynamic conductance of disordered systems

For a system consisting of a scattering region and two leads under ac bias, the Hamiltonian can be written as ($e = 1$ and $\hbar = 1$)

$$H = H_0 + V + H_{leads} + H_T. \tag{1}$$

The first two terms describe the Hamiltonians of the central region (H_0) and the isolated leads (H_{leads}), with

$$H_0 = \sum_m \epsilon_m d_m^\dagger d_m \tag{2}$$

and

$$H_{leads} = \sum_{k\alpha} \epsilon_{k\alpha} c_{k\alpha}^\dagger c_{k\alpha}, \tag{3}$$

where $d_n^\dagger$ and $c_{k\alpha}^\dagger$ ($\alpha = L, R$ is the lead index) are the creation operators of electrons in the scattering region and leads, respectively. In the presence of the disorder potential, we use V to denote the on-site disorder potential. The hopping between the scattering region and leads H_T is represented by the last term with the coupling strength $t_{k\alpha n}$,

$$H_T = \sum_{k\alpha,n} (t_{k\alpha,n} c_{k\alpha}^\dagger d_n + t_{k\alpha,n}^* d_n^\dagger c_{k\alpha}). \tag{4}$$

Under ac bias, the single-particle energy in the leads is given by $\epsilon_{k\alpha}(t) = \epsilon_{k\alpha}^0 + v_\alpha \cos(\Omega t)$, where $\epsilon_{k\alpha}^0$ describes the time-independent equilibrium energy. The equilibrium retarded Green's function of this system is defined as

$$G^r(E) = \frac{1}{E - H_0 - V - \Sigma^r}, \tag{5}$$

where Σ^r is the self-energy due to the presence of leads.

When the bias voltage is small, the frequency-dependent conductance is given by [16]

$$G_{\alpha\beta}(\Omega) = \int \frac{dE}{2\pi} \frac{f - \bar{f}}{\Omega} \mathrm{Tr}[\bar{G}^r \Gamma_\beta G^a (\Gamma_\alpha - \Gamma \delta_{\alpha\beta} + i\Omega \delta_{\alpha\beta})], \tag{6}$$

where $\bar{G}^r(E) = G^r(E_+)$, $E_+ = E + \Omega$, f is the Fermi distribution function, $\bar{f} = f(E_+)$, $\alpha, \beta = L, R$, and $\Gamma = -2\mathrm{Im}\Sigma^r$ is the linewidth function due to the leads.

We wish to calculate the disorder-averaged frequency-dependent or dynamic conductance within the CPA. This amounts to taking the disorder average of two Green's functions with different energies, i.e., calculating $\langle \bar{G}^r \Gamma_\beta G^a \rangle$, where $\langle \cdot \rangle$ stands for the disorder average. The method of nonequilibrium vortex correction, which works well for two Green's functions with the same energy, cannot be used here [45–47]. As will be demonstrated below, it is very convenient to use an approach very similar to the FCS-CPA method [58]. In this approach, a new Green's function $\mathcal{G}$ with the dimension twice the original Green's function is introduced. Based on this new Green's function, there is no need to perform the

average of the two Green's functions; the CPA of a single $\mathcal{G}$ is enough.

In order to do this, we first design a CGF with a counting field such that its first derivative with respect to the counting field gives the expected disorder-averaged dynamic conductance. The following definition of the CGF gives the desired result:

$$\ln Z_{\alpha\beta}(\lambda) = \int \frac{dE}{2\pi}\frac{f-\bar{f}}{\Omega}\mathrm{Tr}\ln[I + G(E)\mathcal{A}_{\alpha\beta}(E)], \quad (7)$$

where λ is the counting field and $\mathcal{A}$ and the generalized Green's function G are defined as

$$\mathcal{A}_{\alpha\beta}(E) = \mathcal{A}_{0,\alpha\beta}(E)\zeta, \quad (8)$$

$$\mathcal{A}_{0,\alpha\beta}(E) = \begin{pmatrix} 0 & -\Gamma_\beta \\ \Gamma_\alpha - \Gamma\delta_{\alpha\beta} + i\Omega I\delta_{\alpha\beta} & 0 \end{pmatrix}, \quad (9)$$

$$G(E) = \begin{pmatrix} \bar{G}^r(E) & 0 \\ 0 & G^a(E) \end{pmatrix}, \quad (10)$$

where $\zeta = \sqrt{e^{i\lambda}-1}$. It is straightforward to show that the first derivative of $\ln Z_{\alpha\beta}(\lambda)$ with respect to $i\lambda$ gives Eq. (6) (see Appendix A).

In the following, we will focus on calculating the dynamic conductance G_{LL}. Using the relation

$$\mathrm{Tr}\ln(I + G\mathcal{A}_{LL}) = \mathrm{Tr}\left(\int_0^1 \frac{dx}{G^{-1} + \mathcal{A}_{LL}x}\mathcal{A}_{LL}\right), \quad (11)$$

the CGF, i.e., $\ln Z_{LL}(\lambda)$, can be expressed as

$$\ln Z_{LL}(\lambda) = \int \frac{dE}{2\pi}\frac{f-\bar{f}}{\Omega}\mathrm{Tr}\left(\int_0^1 dx\, \mathcal{G}(x)\mathcal{A}_{LL}\right), \quad (12)$$

where the new Green's function $\mathcal{G}(x) = (G^{-1} + \mathcal{A}_{LL}x)^{-1}$ is defined in order to perform the disorder average within the CPA. The averaged CGF $\langle \ln Z\rangle$ is finally obtained:

$$\langle \ln Z_{LL}\rangle = \int \frac{dE}{2\pi}\frac{f-\bar{f}}{\Omega}\mathrm{Tr}\left(\int_0^1 dx\, \langle\mathcal{G}(x)\rangle\mathcal{A}_{LL}\right), \quad (13)$$

where the averaged Green's function $\langle\mathcal{G}(x)\rangle$ can be calculated from the CPA method discussed in Ref. [58], from which we have

$$\langle\mathcal{G}(x)\rangle = \left(G_0^{-1} + \mathcal{A}_{LL}x - \Delta\mathcal{E}\right)^{-1}, \quad (14)$$

where G_0 and $\Delta\mathcal{E}$ are given by

$$G_0 = \begin{pmatrix} \bar{G}_0^r & 0 \\ 0 & G_0^a \end{pmatrix}, \quad (15)$$

$$\Delta\mathcal{E} = \begin{pmatrix} \Delta\mathcal{E}_{11} & \Delta\mathcal{E}_{12} \\ \Delta\mathcal{E}_{21} & \Delta\mathcal{E}_{22} \end{pmatrix}. \quad (16)$$

Here $\Delta\mathcal{E}_{ij}$ $(i,j=1,2)$ is a subblock matrix of $\Delta\mathcal{E}$ and is diagonal, and $G_0^r = 1/(E - H_0 - \Sigma^r)$ is the retarded Green's function of the clean system. The renormalized on-site potential (2×2 matrix) for the CGF $\Delta\mathcal{E}^{ii}$ is determined by

$$\Delta\mathcal{E}^{ii} = \int dv^{ii}\rho(v^{ii})v^{ii}[I - \langle\mathcal{G}(x)\rangle^{ii}(v^{ii}I - \Delta\mathcal{E}^{ii})]^{-1}, \quad (17)$$

where $\langle\mathcal{G}(x)\rangle^{ii}$ is a 2×2 submatrix of $\langle\mathcal{G}(x)\rangle$, v^{ii} is the random on-site potential, and $\rho(v^{ii})$ is the distribution of v^{ii}.

Note that the integral of x in Eq. (13) can be avoided in the numerical calculation because the quantities of interest involve at least a first-order derivative. Due to the fact that $\mathcal{G} = \mathcal{G}(\zeta x)$, we have

$$\frac{\partial\langle\ln Z_{LL}\rangle}{\partial i\lambda} = \frac{e^{i\lambda}}{\sqrt{e^{i\lambda}-1}}\int\frac{dE}{4\pi}\frac{f-\bar{f}}{\Omega}\mathrm{Tr}[\langle\mathcal{G}(\zeta)\rangle\mathcal{A}_{0,LL}], \quad (18)$$

where $\mathcal{G}(\zeta) = \mathcal{G}(\zeta x)|_{x=1}$. Then the first-order derivative can be calculated numerically using Eq. (18) by setting $i\lambda$ to a small number.

To summarize the calculational procedure, we first solve $\Delta\mathcal{E}$ from Eq. (17), which depends on λ through matrix $\mathcal{A}_{LL}$ defined in Eq. (8). Then we calculate the disorder-averaged Green's function $\langle\mathcal{G}(x)\rangle$ from Eq. (14). Finally, the dynamic conductance $\langle G_{LL}\rangle$ is obtained from Eq. (18). Note that in deriving the ac conductance, the wideband limit has been used. For instance, the quantity $\partial_E\Gamma$ has been neglected. However, once the formula is derived, the linewidth function Γ appearing in the formula does depend on E. At this level, Eq. (6) is equivalent to the scattering matrix theory. To simplify the discussion, we consider only the case of zero temperature. At finite temperatures, the Fermi distribution function enters in the formula. We will get qualitatively the same physics. Concerning the ac bias, the adiabatic approximation has been used, so that the frequency should not be too much higher than THz.

B. Frequency-dependent shot noise under dc bias for disordered systems

For a system with dc bias, we use the same Hamiltonian as in Eq. (1) by setting the frequency of the ac bias $\Omega = 0$. The current correlation function under dc bias is defined as [11]

$$2S_{\alpha\beta}(t-t') = \langle\Delta\hat{I}_\alpha(t)\Delta\hat{I}_\beta(t') + \Delta\hat{I}_\beta(t')\Delta\hat{I}_\alpha(t)\rangle, \quad (19)$$

where $\Delta\hat{I}_\alpha(t) = \hat{I}_\alpha(t) - \langle\hat{I}_\alpha(t)\rangle$ and $\hat{I}_\alpha(t)$ is the current operator. Note that under dc bias, the average current $\langle\hat{I}_\alpha(t)\rangle$ is independent of time, while the current correlation $S_{\alpha\beta}$ does depend on time [11]. Taking the Fourier transform, we obtain the frequency-dependent noise spectrum,

$$2\pi\delta(\omega+\omega')S_{\alpha\beta}(\omega) = \langle\Delta\hat{I}_\alpha(\omega)\Delta\hat{I}_\beta(\omega') + \Delta\hat{I}_\beta(\omega')\Delta\hat{I}_\alpha(\omega)\rangle.$$

We are interested in the frequency-dependent noise spectrum in the linear response regime and need to derive its analytic expression. To make the presentation simpler, we will use scattering matrix theory to calculate the noise spectrum and then use the Fisher-Lee relation [59] to express the final results in terms of the nonequilibrium Green's function. The frequency-dependent current operator within scattering matrix theory is given by [11]

$$\hat{I}_\alpha(\omega) = \int\frac{dE}{2\pi}\sum_{\beta\gamma}\hat{a}_\beta^\dagger(E)\hat{a}_\gamma(\bar{E})A_{\beta\gamma}(\alpha,E,\bar{E}), \quad (20)$$

where $a_\beta^\dagger$ is the creation operator for the electron incident from lead β, $\bar{E} = E + \omega$, and the matrix A is defined as [60]

$$A_{\beta\gamma}(\alpha,E,\bar{E}) = \delta_{\alpha\beta}\delta_{\alpha\gamma} - s_{\alpha\beta}^\dagger(E)s_{\alpha\gamma}(\bar{E}), \quad (21)$$

where $s^{\dagger}_{\alpha\beta}(E)$ is the scattering matrix from lead β to lead α. It was found that [11]

$$S_{\alpha\beta}(\omega) = \int \frac{dE}{2\pi} \sum_{\gamma\delta} A_{\gamma\delta}(\alpha, E, \bar{E}) A_{\delta\gamma}(\beta, \bar{E}, E) F_{\gamma\delta}(E, \bar{E}), \tag{22}$$

where

$$F_{\gamma\delta}(E, \bar{E}) = f_{\gamma}(E)[1 - f_{\delta}(\bar{E})] + f_{\delta}(\bar{E})[1 - f_{\gamma}(E)]. \tag{23}$$

In the linear response regime at zero temperature, the frequency-dependent shot noise under dc bias is found to be (see Appendix B)

$$2\pi S_{LL}(\omega) = \mathrm{Tr}[(\hat{T}_{+} - \hat{T}_{-})\hat{T}]v, \tag{24}$$

where we have used E instead of E_F. Here $\hat{T}_{+} = \hat{T}(E + \omega)$, $\hat{T}_{-} = \hat{T}(E - \omega)$, v is the voltage difference between two leads, and $\hat{T} = G^{a}\Gamma_R G^{r}\Gamma_L$. For simplicity, we shall discuss $S'_{LL}(\omega) = 2\pi S_{LL}/v$ in the following.

From Eq. (24), we see that to obtain the disorder-averaged frequency-dependent shot noise we have to calculate the disorder average of four Green's functions at different energies. In the following, we discuss how to calculate $\mathrm{Tr}[\hat{T}(E_{+})\hat{T}(E)]$. The idea is to construct the following generalized Green's function G using the four Green's functions G^{a}, $\bar{G}^{a}$, $\bar{G}^{r}$, G^{r}:

$$G = \begin{pmatrix} \bar{G}^{r} & 0 & 0 & 0 \\ 0 & G^{r} & 0 & 0 \\ 0 & 0 & \bar{G}^{a} & 0 \\ 0 & 0 & 0 & G^{a} \end{pmatrix}, \tag{25}$$

with

$$A = \begin{pmatrix} 0 & 0 & 0 & \bar{\Gamma}_L \\ 0 & 0 & \Gamma_L & 0 \\ -\bar{\Gamma}_R & 0 & 0 & 0 \\ 0 & -\Gamma_R & 0 & 0 \end{pmatrix}. \tag{26}$$

We will show below that taking derivatives of the following generating function can give rise to the quantity $\mathrm{Tr}(\hat{T}_{+}\hat{T})$:

$$\begin{aligned} Z &= \mathrm{Det}[I + GA\zeta] \\ &= \mathrm{Det}\begin{pmatrix} I & 0 & 0 & \bar{G}^{r}\bar{\Gamma}_L\zeta \\ 0 & I & G^{r}\Gamma_L\zeta & 0 \\ -\bar{G}^{a}\bar{\Gamma}_R\zeta & 0 & I & 0 \\ 0 & -G^{a}\Gamma_R\zeta & 0 & I \end{pmatrix}. \end{aligned} \tag{27}$$

From the relation

$$\mathrm{Det}\begin{pmatrix} a & b \\ c & d \end{pmatrix} = \mathrm{Det}(a)\mathrm{Det}(d - ca^{-1}b), \tag{28}$$

we find

$$\begin{aligned} \ln Z &= \ln \mathrm{Det}\left[I + \begin{pmatrix} \bar{G}^{a}\bar{\Gamma}_R & 0 \\ 0 & G^{a}\Gamma_R \end{pmatrix}\begin{pmatrix} 0 & \bar{G}^{r}\bar{\Gamma}_L \\ G^{r}\Gamma_L & 0 \end{pmatrix}\zeta^2\right] \\ &= \mathrm{Tr}\ln\left[I + B\zeta^2\right], \end{aligned} \tag{29}$$

where

$$B = \begin{pmatrix} 0 & \bar{G}^{a}\bar{\Gamma}_R\bar{G}^{r}\bar{\Gamma}_L \\ G^{a}\Gamma_R G^{r}\Gamma_L & 0 \end{pmatrix} = \begin{pmatrix} 0 & \hat{T}_{+} \\ \hat{T} & 0 \end{pmatrix}.$$

Expanding Eq. (29) in terms of $z = \zeta^2 = \exp(i\lambda) - 1$, we have

$$\begin{aligned} \ln Z &= \mathrm{Tr}[Bz - (1/2)B^2z^2 - \cdots] \\ &= \mathrm{Tr}[-\hat{T}\hat{T}_{+}z^2 + \cdots]. \end{aligned} \tag{30}$$

Focusing on the second order in z, we can calculate the second-order derivative of $\ln Z$,

$$\frac{\partial^2 \ln Z}{\partial(i\lambda)^2}|_{\lambda=0} = 2\mathrm{Tr}[\hat{T}_{+}\hat{T}], \tag{31}$$

which gives the desired quantity $\mathrm{Tr}[\hat{T}_{+}\hat{T}]$. Similarly, $\mathrm{Tr}[\hat{T}(E_{-})\hat{T}(E)]$ can be calculated by changing ω to a negative value. Finally, one can calculate the frequency-dependent shot noise in clean systems as defined in Eq. (24). In order to calculate the disorder-averaged shot noise within the CPA, we shall discuss how to calculate the disorder-averaged generating function $\langle \ln Z \rangle$ defined in Eq. (27) in the following. We note that Eq. (27) can be expressed as [see Eq. (11)]

$$\langle \ln Z \rangle = \mathrm{Tr}\left(\int_0^1 dx\, \langle \mathcal{G}(x) \rangle A\right), \tag{32}$$

where G and A are defined in Eqs. (25) and (26). The Green's function $\mathcal{G}(x) = (G^{-1} + Ax)^{-1}$ is defined in order to perform the disorder average within the CPA,

$$\langle \mathcal{G}(x) \rangle = \left(G_0^{-1} + Ax - \Delta\mathcal{E}\right)^{-1}. \tag{33}$$

Note that G_0 and $\Delta\mathcal{E}$ are 4 by 4 block matrices,

$$G_0 = \begin{pmatrix} \bar{G}_0^{r} & 0 & 0 & 0 \\ 0 & G_0^{r} & 0 & 0 \\ 0 & 0 & \bar{G}_0^{a} & 0 \\ 0 & 0 & 0 & G_0^{a} \end{pmatrix}, \tag{34}$$

$$\Delta\mathcal{E} = \begin{pmatrix} \Delta\mathcal{E}_{11} & \Delta\mathcal{E}_{12} & \Delta\mathcal{E}_{13} & \Delta\mathcal{E}_{14} \\ \Delta\mathcal{E}_{21} & \Delta\mathcal{E}_{22} & \Delta\mathcal{E}_{23} & \Delta\mathcal{E}_{24} \\ \Delta\mathcal{E}_{31} & \Delta\mathcal{E}_{32} & \Delta\mathcal{E}_{33} & \Delta\mathcal{E}_{34} \\ \Delta\mathcal{E}_{41} & \Delta\mathcal{E}_{42} & \Delta\mathcal{E}_{43} & \Delta\mathcal{E}_{44} \end{pmatrix}. \tag{35}$$

Here $\Delta\mathcal{E}_{ij}$ $(i, j = 1, \ldots, 4)$ is the subblock matrix of $\Delta\mathcal{E}$ which is diagonal, and $G_0^{r} = 1/(E - H_0 - \Sigma^{r})$ is the retarded Green's function of the pure system. $\Delta\mathcal{E}^{ii}$ can be calculated by using Eq. (17) with $\langle \mathcal{G}(x) \rangle^{ii}$ defined in Eq. (33).

C. Frequency-dependent noise spectrum under ac bias for disordered systems

For a system under ac bias, the current correlation function under ac bias is defined as [11]

$$\begin{aligned} S(\Omega) = 4k_bT\,\mathrm{Tr}[\hat{T}^2] + \sum_{\pm}\sum_{n=0}^{\infty} J_l^2\left(\frac{\bar{V}}{\Omega}\right)\mathrm{Tr}[\hat{T}(I - \hat{T})] \\ \times\left[(V \pm n\Omega)\coth\left(\frac{\bar{V} \pm n\Omega}{2k_bT}\right)\right], \end{aligned} \tag{36}$$

where k_b is the Boltzmann constant, T is temperature, J_l is the Bessel function, and $\hat{T}(E_f) = G^{a}\Gamma_R G^{r}\Gamma_L$ is the transmission matrix evaluated at the Fermi energy E_f of the system. Here we suppose that $\bar{V} = v_L$ and v_R is equal to zero. It is worth mentioning that the first term in Eq. (36) is thermal noise, while the second term is the shot noise due to solely the bias.

In order to calculate the disorder-averaged frequency-dependent noise spectrum $\langle S(\Omega)\rangle$ under ac bias, one needs to know only two disorder-averaged dc quantities, $\langle \hat{T}\rangle$ and $\langle \hat{T}^2\rangle$, and other quantities are irrelevant in disorder configurations. According to Ref. [58], we know that they can be calculated by disorder-averaged first- and second-order cumulants,

$$\langle \hat{T}\rangle = \langle C_1\rangle, \quad \langle \hat{T}^2\rangle = \langle C_1\rangle - \langle C_2\rangle, \tag{37}$$

where

$$\langle C_n\rangle = \frac{\partial^n \langle \ln Z\rangle}{\partial (i\lambda)^n}|_{\lambda=0}, \quad \langle \ln Z\rangle = \mathrm{Tr}\left(\int_0^1 dx\, \langle \mathcal{G}(x)\rangle A\right). \tag{38}$$

Here $\mathcal{G}(x)$ and A are defined as

$$\langle \mathcal{G}(x)\rangle = \left(G_0^{-1} + Ax - \Delta\mathcal{E}\right)^{-1},$$
$$A = \begin{pmatrix} 0 & -\Gamma_R \\ \Gamma_L & 0 \end{pmatrix}\zeta, \tag{39}$$

where we have introduced

$$G_0 = \begin{pmatrix} G_0^r & 0 \\ 0 & G_0^a \end{pmatrix}, \quad \Delta\mathcal{E} = \begin{pmatrix} \Delta\mathcal{E}_{11} & \Delta\mathcal{E}_{12} \\ \Delta\mathcal{E}_{21} & \Delta\mathcal{E}_{22} \end{pmatrix}. \tag{40}$$

Note that $G_0^r = [G^a]^\dagger = 1/(E - H_0 - \Sigma^r)$ is still the retarded Green's function of the pure system. Once $\Delta\mathcal{E}^{ii}$ are obtained self-consistently by using Eq. (17) with $\langle \mathcal{G}(x)\rangle^{ii}$ defined in Eq. (39), the disorder-averaged generating function $\langle \ln Z\rangle$ and hence the cumulants $\langle C_n\rangle$ can be calculated.

To end this section, we note that the above theoretical formalisms can be easily implemented and applied to study the Anderson disorder or the binary type of disorders. The numerical results calculated using this formalism will be presented in the next section.

III. NUMERICAL RESULTS

As an application, we have implemented our formalism in the tight-binding model on the two-dimensional square-lattice system. In the tight-binding model, the hopping energy between the nearest lattice sites is set to be $t = 1$, and the on-site energy is 4. In the numerical simulation, the central scattering region system has 30×30 sites. Anderson disorder will be considered in the numerical simulation. For the Anderson type of disorder, the disorder distribution function $\rho(v^{ii})$ is defined as

$$\rho(v^{ii}) = \begin{cases} 1/\mathrm{W}, & -\mathrm{W}/2 \leqslant v^{ii} \leqslant \mathrm{W}/2, \\ 0, & \text{otherwise}, \end{cases} \tag{41}$$

where W denotes the disorder strength. During the brute force calculation, the dynamic conductance and frequency-dependent noise spectrum under ac bias are averaged over 1000 configurations, while the frequency-dependent shot noise under dc bias is averaged over 100 000 configurations due to its large fluctuation over the configuration average.

A. Dynamic conductance

In this section, we will show the numerical results of dynamic conductance $\langle G_{LL}\rangle$ for the Anderson disorder within a wide range of disorder strengths W (from 0.01 to 3). In Fig. 1, the disorder-averaged dynamic conductance $\langle G_{LL}\rangle$ versus the disorder strength W is presented. Here the Fermi energy and frequency are chosen to be $E_f = 0.3$ and $\Omega = 0.1, 0.2$ as an illustration. Since dynamic conductance is a complex quantity, the real and imaginary parts are plotted separately. At first glance, we see that the brute force results and FCS-CPA results agree remarkably well for both real and imaginary parts. However, we do see that some deviation between results for brute force and the FCS-CPA gradually increases as the disorder strength W increases. This is understandable since in the CPA we have neglected some of the multiple-scattering terms which play an important role at large disorder strengths. Furthermore, we note that the magnitude of the real (imaginary) part gradually decreases (increases) with increasing of disorder strength. In contrast to the $\Omega = 0.2$ case, the imaginary part of $\langle G_{LL}\rangle$ in the $\Omega = 0.1$ case starts from a positive value.

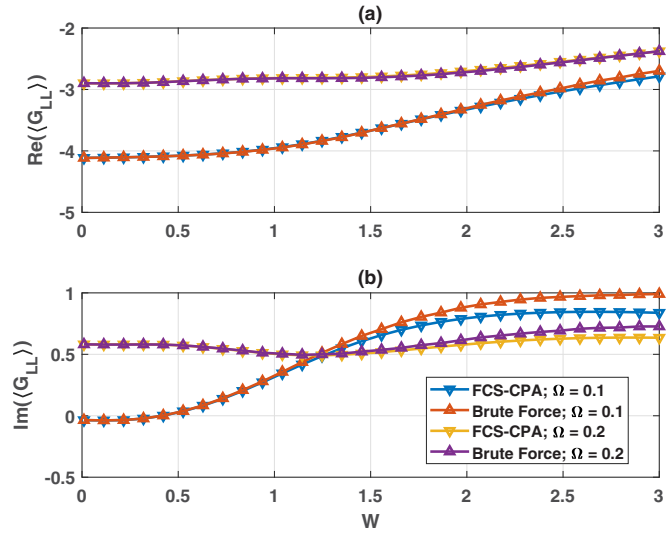

FIG. 1. (a) The real and (b) imaginary parts of disorder-averaged dynamic conductance $\langle G_{LL}\rangle$ versus the disorder strength W. Here the Fermi energy and frequency are chosen to be $E_f = 0.3$, $\Omega = 0.1, 0.2$. One thousand configurations were calculated and averaged in the brute force calculation.

To demonstrate the feature of the disorder effect on the dynamic conductance G_{LL} in a wide range of frequencies and Fermi energies, we have calculated the phase diagram for $\langle G_{LL}\rangle$ in Fig. 2. In view of the remarkable agreement between brute force and the FCS-CPA, we use the FCS-CPA method to calculate $\langle G_{LL}\rangle$ in the (Ω, W) and (E_f, W) planes to avoid the huge computational burden of the brute force calculation. As shown in Fig. 2(a), the real part of $\langle G_{LL}\rangle$ increases when the frequency increases in the small-disorder-strength region. Compared with the frequency dependence phase diagram, the real part of $\langle G_{LL}\rangle$ increases with the Fermi energy in Fig. 2(c). For the imaginary part, similar behavior can be found in the large-disorder-strength region. It is interesting that the real part of the dynamic conductance is monotonously decreasing in the entire region of E_f and Ω as disorder strength W increases. However, the imaginary part first decreases as disorder strength increases and then increases a little bit again.

Furthermore, we also calculate the disorder-averaged dynamic conductance G_{LL} in the (Ω, E_f) plane by using the

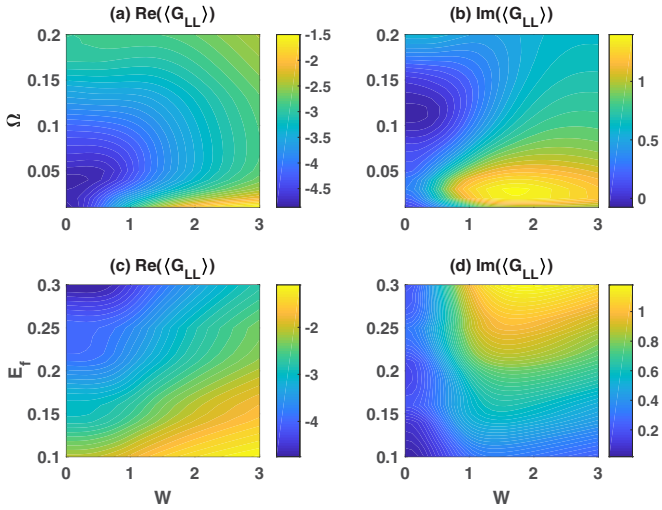

FIG. 2. (a) The real and (b) imaginary parts of the calculated phase diagram for disorder-averaged dynamic conductance $\langle G_{LL}\rangle$ in the (Ω, W) plane. Here the Fermi energy is fixed as $E_f = 0.3$. (c) The real and (d) imaginary parts of the calculated phase diagram for disorder-averaged dynamic conductance $\langle G_{LL}\rangle$ in the (E_f, W) plane. Here the frequency is fixed as $\Omega = 0.05$.

FCS-CPA method. The numerical results are presented in Fig. 3. As an example, we chose two disorder strengths, $W = 0.5, 1.5$. At first glance, we see that the real part of G_{LL} shows nearly the same pattern in the whole range of Ω and E_f. The magnitude of the real part for $W = 1.5$ is smaller than that of $W = 0.5$ if we consider the same point (Ω, E_f) in the phase diagram. However, for the imaginary part, as shown in Figs. 3(c) and 3(d), it oscillates with the Fermi energy if we fix the frequency. For the $W = 0.5$ case, the imaginary part first increases with the Fermi energy, then decreases, and finally increases.

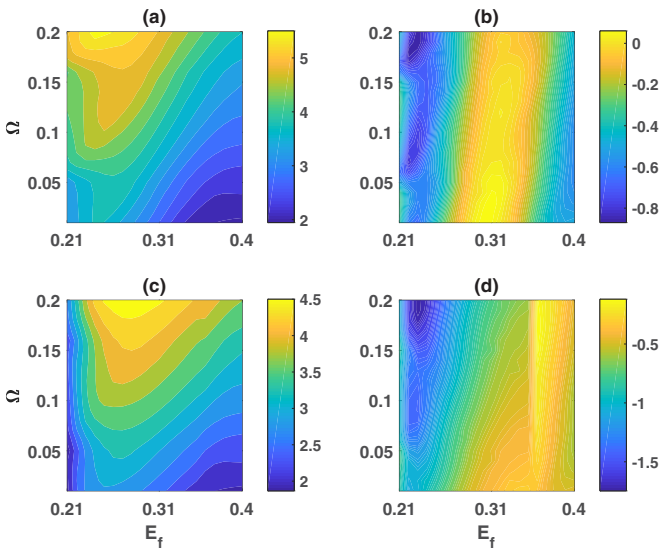

FIG. 3. The (a) and (c) real and (b) and (d) imaginary parts of the calculated phase diagram for disorder-averaged dynamic conductance $\langle G_{LL}\rangle$ in the (Ω, E_f) plane. Here the disorder strength is fixed as $W = 0.5$ for (a) and (b) and $W = 1.5$ for (c) and (d).

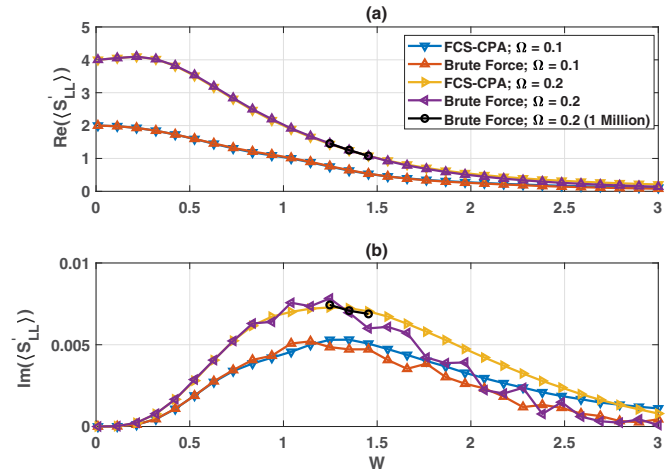

FIG. 4. (a) The real and (b) imaginary parts of disorder-averaged frequency-dependent shot noise $\langle S'_{LL}(\omega)\rangle$ versus the disorder strength W. Here the Fermi energy and frequency are chosen to be $E_f = 0.3$, $\omega = 0.1, 0.2$. One hundred thousand configurations were calculated and averaged in the brute force calculations for the red line with upward triangle and purple line with the left-pointing triangle. One million configurations were calculated to check the convergence (black line with circles).

B. Frequency-dependent shot noise under dc bias

In this section, the numerical results for the frequency-dependent shot noise $\langle S'_{LL}(\omega)\rangle$ are presented. In Fig. 4, we plot the numerical results of the brute force calculation and of the FCS-CPA method. Here the Fermi level is also chosen to be $E_f = 0.3$. Before analyzing the disorder-averaged case, we briefly discuss the frequency-dependent shot noise in the clean limit. When disorder strength $W = 0$, $S'_{LL}(\omega) = \mathrm{Tr}[(\hat{T}_+ - \hat{T}_-)\hat{T}]$ is an integer that is determined by the channel number $N(E) = T(E)$ difference between energy $E + \omega$ and $E - \omega$.

From Fig. 4, we see that the real parts of $\langle S'_{LL}(\omega)\rangle$ for brute force and FCS-CPA calculations agree remarkably well in the whole disorder strength range. However, for the imaginary parts of the brute force calculation it is very difficult to converge at large W ($W > 0.9$) even if it is averaged using 100 000 configurations. To check the convergence, 1×10^6 configurations were calculated, which is very costly, for three disorder strength points, as shown in Fig. 4. Compared with imaginary parts averaged using 10 000 configurations, the corresponding results with 1×10^6 configurations are smoother and close to the FCS-CPA results in the middle range of disorder strength. As disorder strength increases, it is found that the imaginary part of the shot noise (FCS-CPA results) starts from zero and reaches its maximum values between $W = 1$ and $W = 2$. Finally, they gradually reduce to zero as the disorder strength further increases. Actually, the imaginary part of the shot noise comes from the disorder-scattering-induced mode mixing in the system. More interestingly, the real part of $\langle S'_{LL}(\omega = 0.2)\rangle$ first increases a little bit versus disorder strength W compared with the $\langle S'_{LL}(\omega = 0.1)\rangle$ case and then begins to decrease as disorder strength increases.

Different from the case of ac bias where there is an intrinsic driving frequency, the frequency-dependent shot noise $S'_{LL}(\omega)$

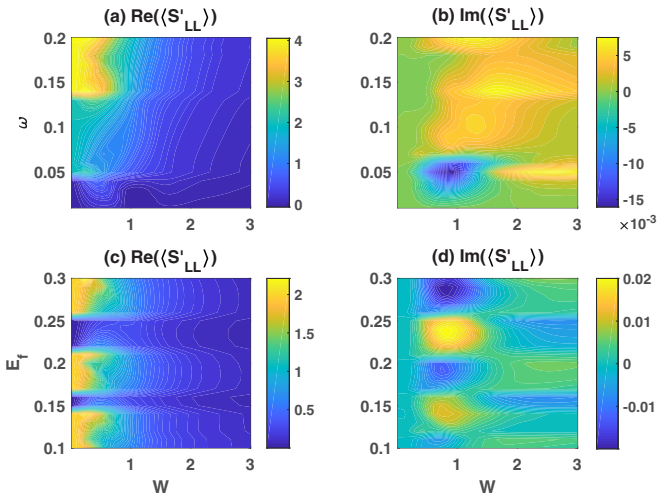

FIG. 5. (a) The real and (b) imaginary parts of the calculated phase diagram for disorder-averaged frequency-dependent shot noise $\langle S'_{LL}\rangle$ in the (ω, W) plane. Here the Fermi energy is fixed as $E_f = 0.3$. (c) The real and (d) imaginary parts of the calculated phase diagram for disorder-averaged frequency-dependent shot noise $\langle S'_{LL}\rangle$ in the (E_f, W) plane. Here the frequency is fixed as $\omega = 0.05$.

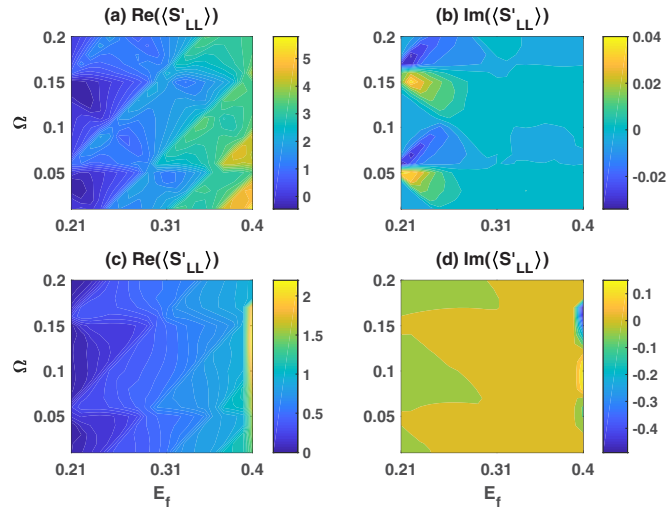

FIG. 6. The (a) and (c) real and (b) and (d) imaginary parts of the calculated phase diagram for disorder-averaged frequency-dependent shot noise $\langle S'_{LL}\rangle$ in the (Ω, E_f) plane. Here disorder strength is fixed as $W = 0.5$ for (a) and (b) and $W = 1.5$ for (c) and (d).

under dc bias is just the Fourier transform of $S'_{LL}(t)$, and the frequency here is a parameter. Note that $S'_{LL}(t)$ is a real quantity; it is easy to confirm that $S'_{LL}(\omega)$ is an odd function of frequency giving rise to a real inverse Fourier transform $S'_{LL}(t)$. The real part of $S'_{LL}(\omega)$ is $\int S'_{LL}(t)\cos(\omega t)dt$, and the imaginary part of $S'_{LL}(\omega)$ is $\int S'_{LL}(t)\sin(\omega t)dt$. Both components are needed in order to describe $S'_{LL}(t)$, and there is no restriction on the imaginary component.

According to Eq. (24), the frequency-dependent shot noise is composed of the correlation of the transmission matrix $\hat{T}$ between electrons at the Fermi energy and above or below the Fermi energy $\hat{T}_{\pm}$. Note that the transmission matrix $\hat{T}$ is Hermitian with real diagonal matrix elements. Hence, if the transmission matrix is diagonal, the frequency-dependent shot noise is real from Eq. (24). The physical meaning of a diagonal transmission matrix is that there is no mode mixing in the transport process: that is, transmission channels n, m are all independent. When there is no mode mixing in the transport, the system behaves one-dimensional. Our system is set up as a quasi-one-dimensional system in the clean limit. That is the reason why the imaginary part of the frequency-dependent shot noise is zero in the clean limit. In the presence of disorders, the scattering events lead to mode mixing, and the transmission matrix becomes complex. The mode mixings or scatterings above and below the Fermi energy are different, leading to a nonzero imaginary part of the frequency-dependent shot noise. In Appendix C, we analytically show that the imaginary part of the transmission matrix element is nonzero and hence the shot noise when there is a Δ potential impurity in the two-dimensional system.

The phase diagrams of the disorder-averaged frequency-dependent shot noise $\langle S'_{LL}\rangle$ in the (E_f, W) and (ω, W) planes are presented in Fig. 5. When disorder strength W is small, the real parts of $\langle S'_{LL}(E_f, W)\rangle$ increase from 1 to 4 when frequency ω changes from 0.01 to 0.2, as shown in Fig. 5(a). As disorder strength increases, they approach zero (blue region). Interestingly, the imaginary parts of $\langle S'_{LL}(E_f, W)\rangle$ can be either positive or negative in Fig. 5(b). With the Fermi energy fixed, we further studied $\langle S'_{LL}(\omega, W)\rangle$. From Fig. 5(c), we can see that the real parts of $\langle S'_{LL}\rangle$ oscillate between 1 and 2 when disorder strength W is small (around 0.2). Similarly, its imaginary parts also have oscillations when W is around 1.

Finally, we also calculated $\langle S'_{LL}\rangle$ in the (Ω, E_f) plane by using the FCS-CPA method. For simplicity, the cases for two disorder strengths, $W = 0.5, 1.5$, are chosen and presented in Fig. 6. The real parts of $\langle S'_{LL}\rangle$ have nearly the same pattern for the two disorder strengths in Figs. 6(a) and 6(c), while the imaginary part of the shot noise is quite different in Figs. 6(b) and 6(d). The imaginary parts are nearly equal to 0.1 in a wide range of the Fermi energy and frequency when $W = 1.5$.

C. Frequency-dependent noise spectrum under ac bias

In this section, we present the numerical results of the disorder-averaged frequency-dependent noise spectrum under ac bias using the FCS-CPA method compared with the brute force calculation. In the numerical simulation, we have fixed the Fermi energy $E_f = 0.3$ and bias amplitude $\bar{V} = 0.2$. The temperature k_bT is in units of hopping energy $t = 1$. To understand how the noise spectrum depends on temperature, we take $k_bT = 0.0001, 0.01$ as an example. Figure 7(a) shows the numerical results of $S(\Omega)$ using the FCS-CPA method and brute force calculations. We can clearly see that the numerical results from both methods agree well in the whole disorder strength range. When $k_bT = 0.0001$, the noise spectrum starts near the zero point compared with the finite value when $k_bT = 0.01$. Since there are two terms in Eq. (36), only the first term depends on temperature. The second term is equal to zero due to the Fermi statistics of electrons ($\mathrm{Tr}[\hat{T}(I - \hat{T})]$) in it when $W = 0$. In Fig. 7(a) when temperature is very low ($k_bT = 0.0001$), the thermal noise is negligible. Hence, the difference in the two curves in Fig. 7(a) mainly comes from

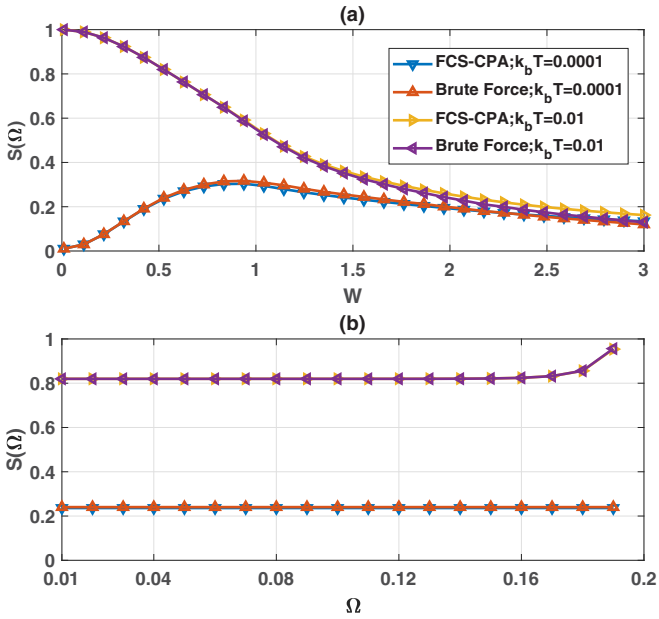

FIG. 7. (a) The disorder-averaged frequency-dependent noise spectrum $\langle S(\Omega)\rangle$ versus the disorder strength W where frequency Ω is fixed as 0.01. (b) The disorder-averaged frequency-dependent noise spectrum $\langle S(\Omega)\rangle$ versus the frequency Ω where disorder strength W is fixed as 0.05. Here the Fermi energy and bias amplitude are chosen as $E_f = 0.3$ and $\bar{V} = 0.2$. One thousand configurations were calculated and averaged in the brute force calculation.

the thermal noise. As the disorder strength increases, the noise spectrum $\langle S(\Omega, k_bT = 0.0001)\rangle$ first increases to a plateau and then decreases. However, $S(\Omega, k_bT = 0.01)$ decreases monotonously as disorder strength increases. In Fig. 7(b), the noise spectrum $\langle S(\Omega)\rangle$ versus the frequency is given by fixing the disorder strength $W = 0.5$. The noise spectrum $\langle S(\Omega, k_bT = 0.0001)\rangle$ remains unchanged in the frequency regime. However, as temperature increases to $k_bT = 0.01$, the noise spectrum remains unchanged first and then increases starting from $\Omega = 0.16$.

IV. SUMMARY

Based on the nonequilibrium Green's function, we have developed a theoretical formalism to calculate the disorder-averaged dynamic conductance, frequency-dependent shot noise under dc bias, and frequency-dependent noise spectrum under ac bias using the FCS framework within the coherent potential approximation. Compared with the numerical calculation method, our FCS-CPA approach provides an effective way to calculate disorder-averaged frequency transport quantities. Without loss of generality, we have implemented our theoretical formalism in the tight-binding model on a square lattice to calculate the three disorder-averaged quantities by considering Anderson-type disorder. From the numerical results, we found that our formalism can give very accurate results compared with the brute force calculation.

ACKNOWLEDGMENTS

This work was financially supported by the National Natural Science Foundation of China (Grants No. 11704232, No. 11434007, No. 11774238), the Research Grant Council (Grant No. 17303418), the University Grant Council (Contract No. AoE/P-04/08) of the government of Hong Kong Special Administrative Region, the National Key R&D Program of China under Grant No. 2017YFA0304203, Changjiang Scholars and Innovative Research Team in University of Ministry of Education of China (Grant No. IRT_17R70), the Shanxi Science and Technology Department (Grant No. 201701D121003), the Shanxi Province 100-Plan Talent Program, and the Fund for Shanxi 1331 Project Key Subjects Construction. This research was conducted using the High Performance Computer of Shanxi University.

APPENDIX A: DYNAMIC CONDUCTANCE

In this Appendix, we will briefly show that the first derivative of $\ln Z_{\alpha\beta}(\lambda)$ with respect to $i\lambda$ gives Eq. (6). By taking the derivative of Eq. (7) and plugging the definitions of $G(E)$ and $\mathcal{A}_{\alpha\beta}(E)$ into Eqs. (8) and (9), we have

$$\begin{aligned}
&\frac{\partial \ln Z_{\alpha\beta}}{\partial(i\lambda)}|_{\lambda=0} \\
&= \frac{\partial}{\partial(i\lambda)}\left\{\int \frac{dE}{2\pi}\frac{f-\bar{f}}{\Omega}\mathrm{Tr}\ln[I + G(E)\mathcal{A}_{\alpha\beta}(E)]\right\}|_{\lambda=0} \\
&= \int \frac{dE}{2\pi}\frac{f-\bar{f}}{\Omega}\frac{\partial}{\partial(i\lambda)}\{\ln \mathrm{Det}[I + \bar{G}^r(E)\Gamma_\beta G^a(E) \\
&\quad \times (\Gamma_\alpha - \Gamma\delta_{\alpha\beta} + i\Omega I\delta_{\alpha\beta})\zeta^2]\}|_{\lambda=0} \\
&= \int \frac{dE}{2\pi}\frac{f-\bar{f}}{\Omega}\mathrm{Tr}\left\{\frac{\partial}{\partial(i\lambda)}\ln[I + \bar{G}^r(E)\Gamma_\beta G^a(E) \right. \\
&\quad \left. \times (\Gamma_\alpha - \Gamma\delta_{\alpha\beta} + i\Omega I\delta_{\alpha\beta})(e^{i\lambda} - 1)]|_{\lambda=0}\right\} \\
&= \int \frac{dE}{2\pi}\frac{f-\bar{f}}{\Omega}\mathrm{Tr}[\bar{G}^r(E)\Gamma_\beta G^a(E)(\Gamma_\alpha - \Gamma\delta_{\alpha\beta} + i\Omega I\delta_{\alpha\beta})] \\
&= G_{\alpha\beta}(\Omega), \qquad \text{(A1)}
\end{aligned}$$

where we have used the relation $\mathrm{Tr}\ln[\cdots] = \ln \mathrm{Det}[\cdots]$.

APPENDIX B: FREQUENCY-DEPENDENT DC SHOT NOISE

We start from the formula for frequency-dependent noise power under the dc bias equation (22). Now we calculate S_{LL} for a two-probe system in the linear response regime at zero temperature using Eq. (22). Expanding $F_{\gamma\delta}(E, \bar{E})$ in Eq. (23) up to first order in the voltage and setting $v_L = 0$ and $v_R = v > 0$, we have the following three relations for positive Ω:

$$f_\alpha(E)[1 - f_\alpha(\bar{E})] \sim \omega,$$

which does not contribute to S_{LL} in the linear regime,

$$\int dE\, f_L(E)[1 - f_R(\bar{E})]u(E) = \int_{E_F-\omega-v}^{E_F} u(E)dE,$$

and

$$\int dE\, f_R(E)[1 - f_L(\bar{E})]u(E) = \theta(\omega - v)\int_{E_F-\omega}^{E_F-v} u(E)dE,$$

where we have used the fact that $f_R(E)[1-f_L(E)]=0$ at zero temperature. Using Taylor expansion $u(E)=u(E_0)+u'(E_0)(E-E_0)+\cdots$, we find

$$\int_{E_F-\omega-v}^{E_F} u(E)dE = u(E_F-\omega)(\omega+v) + u'(E_F-\omega)(\omega^2-v^2)+\cdots$$

and

$$\int_{E_F-\omega}^{E_F-v} u(E)dE = u(E_F)(\omega-v)+u'(E_F)(\omega^2-v^2)+\cdots.$$

Hence, in the linear regime, there are only two terms in the summation $\sum_{\gamma\delta}$ in Eq. (22), $\gamma=L,\delta=R$ and $\gamma=R,\delta=L$, with $A_{LR}(L,E,\bar{E})A_{RL}(L,\bar{E},E)=\mathrm{Tr}[s^{\dagger}_{LL}(E)s_{LL}(E)s^{\dagger}_{LR}(\bar{E})s_{LR}(\bar{E})]=\mathrm{Tr}\{[1-\hat{T}(E)]\hat{T}(\bar{E})\}$ and $A_{LR}(L,E,\bar{E})A_{RL}(L,\bar{E},E)=\mathrm{Tr}\{[1-\hat{T}(\bar{E})]\hat{T}(E)\}$, where Tr is over different conducting channels.

We finally have

$$2\pi S_{LL}(\omega)=\mathrm{Tr}\{[1-\hat{T}(E_F-\omega)]\hat{T}(E_F)\} - \theta(\omega-v)\mathrm{Tr}\{[1-\hat{T}(E_F+\omega)]\hat{T}(E_F)\},$$

which recovers the known results $2\pi S_{LL}=\mathrm{Tr}[(1-\hat{T})\hat{T}]$ at $\omega=0$. At finite frequency, we have $\theta(\omega-v)=1$ in the linear response regime. Therefore, we arrive at

$$2\pi S_{LL}(\omega)=\mathrm{Tr}\{[\hat{T}(E_F+\omega)-\hat{T}(E_F-\omega)]\hat{T}(E_F)\}.$$

APPENDIX C: MODE-MIXING-INDUCED IMAGINARY PART OF THE FREQUENCY-DEPENDENT DC SHOT NOISE

In this Appendix, we will analytically show that the imaginary part of the transmission matrix element is nonzero once there is an impurity in the two-dimensional system. As an example, we shall consider a Δ potential impurity in the two-dimensional square-lattice system which is located in the center of the system, i.e., $V(x,y)=V_0\delta(x-L/2)\delta(y-L/2)$. Here we assume that the system length is $L\times L$ with boundaries $x_L=0, x_R=L$. The scattering wave function $\psi_{\alpha m}$ can be calculated by the Lippmann-Schwinger equation with first-order approximation [61],

$$\psi_{\alpha m}=\psi^0_{\alpha m}+G^r_0V\psi_{\alpha m} \simeq \psi^0_{\alpha m}+G^r_0V\psi^0_{\alpha m}, \quad \text{(C1)}$$

where $\psi^0_{\alpha m}$ and G^r_0 are the scattering wave function and Green's function in the clean limit, respectively. They are defined as [61,62]

$$\psi^0_{\alpha m}(x,y)=-i\chi_m(y)e^{ik_m(x-x_\alpha)},$$
$$G^r_0(x,x',y,y')=\sum_m\frac{-i}{\hbar v_m}\chi_m(y)\chi_m(y')e^{ik_m|x-x'|}, \quad \text{(C2)}$$

where $\chi_m(y)$ is the transverse mode function, $v_m=\hbar k_m/m$ is the velocity of the mth mode, and $k_m=\sqrt{2m(E-\epsilon_m)}/\hbar$, with ϵ_m being the threshold of the mth mode. According to the definition of the scattering matrix s_{RLnm} [62], we have

$$\begin{aligned} s_{RLnm} &= i\langle W_{Rm}|\psi_{Ln}\rangle/\kappa_m \\ &= i\langle W_{Rm}|\psi^0_{Ln}\rangle/\kappa_m + i\langle W_{Rm}|G^r_0V\psi^0_{Ln}\rangle/\kappa_m \\ &= \delta_{nm}e^{ik_nL}-\frac{iV_0}{\hbar v_m}e^{i(k_m+k_n)\frac{L}{2}}\chi_m\left(\frac{L}{2}\right)\chi_n\left(\frac{L}{2}\right), \end{aligned} \quad \text{(C3)}$$

where $|W_{\alpha m}(x,y)\rangle$ is the source of the αth lead [61],

$$|W_{\alpha m}(x,y)\rangle=\kappa_m\chi_m(y)\delta(x-x_\alpha), \quad \text{(C4)}$$

where we have introduced $\kappa_m=\sqrt{\hbar v_m}$. From Eq. (C3), we know the second term comes from the scattering event and modes n and m are mixed. Without impurity scattering, the second term is equal to zero, and there is no mode mixing.

Once the scattering matrix is known, we can calculate the transmission matrix element $\hat{T}_{nm}=\sum_l s^*_{RLln}s_{RLlm}$. In the clean limit, we can easily know that $\hat{T}_{nm}$ is diagonal and purely real without mode mixing. In the presence of impurity, the transmission matrix element $\hat{T}_{nm}$ becomes (up to first order in V_0)

$$\hat{T}_{nm}=\delta_{nm}+\frac{iV_0}{\hbar}\left[\frac{1}{v_n}e^{i(k_n-k_m)\frac{L}{2}} - \frac{1}{v_m}e^{i(k_m-k_n)\frac{L}{2}}\right]\chi_m\left(\frac{L}{2}\right)\chi_n\left(\frac{L}{2}\right). \quad \text{(C5)}$$

Note that the off-diagonal terms of the transmission matrix are complex quantities. In order to calculate the frequency-dependent shot noise, $\hat{T}_{nm}$ should be calculated in two different energies $E\pm\Omega$, and the imaginary part cannot be canceled. Finally, we know that the imaginary part of the frequency-dependent shot noise is due to the mode mixing when the disorder is present.

[1] M. Buttiker, J. Phys.: Condens. Matter **5**, 9361 (1993).
[2] M. Buttiker, A. Pretre, and H. Thomas, Phys. Rev. Lett. **70**, 4114 (1993).
[3] G. B. Lesovik and L. S. Levitov, Phys. Rev. Lett. **72**, 538 (1994).
[4] C. Bruder and H. Schoeller, Phys. Rev. Lett. **72**, 1076 (1994).
[5] A. P. Jauho, N. S. Wingreen, and Y. Meir, Phys. Rev. B **50**, 5528 (1994).
[6] A. Schiller and S. Hershfield, Phys. Rev. Lett. **77**, 1821 (1996).
[7] J. C. Cuevas, A. Martin-Rodero, and A. Levy Yeyati, Phys. Rev. B **54**, 7366 (1996).
[8] R. J. Schoelkopf, P. J. Burke, A. A. Kozhevnikov, D. E. Prober, and M. J. Rooks, Phys. Rev. Lett. **78**, 3370 (1997).
[9] R. J. Schoelkopf, A. A. Kozhevnikov, D. E. Prober, and M. J. Rooks, Phys. Rev. Lett. **80**, 2437 (1998).
[10] Q. F. Sun, J. Wang, and T. H. Lin, Phys. Rev. B **61**, 12643 (2000).
[11] Y. M. Blanter and M. Buttiker, Phys. Rep. **336**, 1 (2000).
[12] J. Appenzeller and D. J. Frank, Appl. Phys. Lett. **84**, 1771 (2004).
[13] S. E. Nigg, R. Lopez, and M. Buttiker, Phys. Rev. Lett. **97**, 206804 (2006).

[14] J. Gabelli, G. Feve, J. M. Berroir, B. Placais, A. Cavanna, B. Etienne, Y. Jin, and D. C. Glattli, Science **313**, 499 (2006).
[15] J. Wang, B. G. Wang, and H. Guo, Phys. Rev. B **75**, 155336 (2007).
[16] Y. D. Wei and J. Wang, Phys. Rev. B **79**, 195315 (2009).
[17] B. Wang, Y. J. Yu, L. Zhang, Y. D. Wei, and J. Wang, Phys. Rev. B **79**, 155117 (2009).
[18] M. Sindel, W. Hofstetter, J. von Delft, and M. Kindermann, Phys. Rev. Lett. **94**, 196602 (2005).
[19] L. Zhang, B. Wang, and J. Wang, Phys. Rev. B **86**, 165431 (2012).
[20] J. N. Zhuang, L. Zhang, and J. Wang, AIP Adv. **1**, 042180 (2011).
[21] G. L. Liu, G. M. Zhang, H. Yu, L. W. Jing, L. W. Ai, and Q. Liu, J. Appl. Phys. **121**, 243902 (2017).
[22] T. M. Philip and M. J. Gilbert, Sci. Rep. **7**, 6736 (2017).
[23] Z. Yu and J. Wang, Phys. Rev. B **91**, 205431 (2015).
[24] S. M. Sze and K. N. Kwok, *Physics of Semiconductor Devices*, 3rd ed. (Wiley, New York, 2006).
[25] P. W. Anderson, Phys. Rev. **109**, 1492 (1958).
[26] P. W. Anderson, Phys. Rev. **124**, 41 (1961).
[27] Y. X. Xing, L. Zhang, and J. Wang, Phys. Rev. B **84**, 035110 (2011).
[28] J. Li, R.-L. Chu, J. K. Jain, and S.-Q. Shen, Phys. Rev. Lett. **102**, 136806 (2009).
[29] L. Zhang, J. N. Zhuang, Y. X. Xing, J. Li, J. Wang, and H. Guo, Phys. Rev. B **89**, 245107 (2014).
[30] L. B. Altshuler, Pis'ma Zh. Eksp. Teor. Fiz. **51**, 530 (1985) [JETP Lett. **41**, 648 (1985)].
[31] P. A. Lee and A. D. Stone, Phys. Rev. Lett. **55**, 1622 (1985).
[32] P. A. Lee, A. D. Stone, and H. Fukuyama, Phys. Rev. B **35**, 1039 (1987).
[33] W. Ren, Z. H. Qiao, J. Wang, Q. F. Sun, and H. Guo, Phys. Rev. Lett. **97**, 066603 (2006).
[34] Z. H. Qiao, J. Wang, Y. D. Wei, and H. Guo, Phys. Rev. Lett. **101**, 016804 (2008).
[35] Z. H. Qiao, Y. X. Xing, and J. Wang, Phys. Rev. B **81**, 085114 (2010).
[36] Z. H. Qiao, Y. L. Han, L. Zhang, K. Wang, X. Z. Deng, H. Jiang, S. A. Yang, J. Wang, and Q. Niu, Phys. Rev. Lett. **117**, 056802 (2016).
[37] C. W. J. Beenakker, Rev. Mod. Phys. **69**, 731 (1997).
[38] P. W. Brouwer and M. Büttiker, Europhys. Lett. **37**, 441 (1997).
[39] A. Ossipov, Phys. Rev. Lett. **121**, 076601 (2018).
[40] N. G. van Kampen, *Stochastic Processes in Physics and Chemistry* (Elsevier, Amsterdam, 2007).
[41] P. Soven, Phys. Rev. **156**, 809 (1967).
[42] D. W. Taylor, Phys. Rev. **156**, 1017 (1967).
[43] B. Velicky, Phys. Rev. **184**, 614 (1969).
[44] R. J. Elliott, J. A. Krumhansl, and P. L. Leath, Rev. Mod. Phys. **46**, 465 (1974).
[45] Y. Ke, K. Xia, and H. Guo, Phys. Rev. Lett. **100**, 166805 (2008).
[46] Y. Ke, K. Xia, and H. Guo, Phys. Rev. Lett. **105**, 236801 (2010).
[47] J. Yan and Y. Q. Ke, Phys. Rev. B **94**, 045424 (2016).
[48] A. V. Kalitsov, M. G. Chshiev, and J. P. Velev, Phys. Rev. B **85**, 235111 (2012).
[49] Y. Zhu, L. Liu, and H. Guo, Phys. Rev. B **88**, 205415 (2013).
[50] C. Zhou, X. Chen, and H. Guo, Phys. Rev. B **94**, 075426 (2016).
[51] J. Yan, S. Wang, K. Xia, and Y. Ke, Phys. Rev. B **95**, 125428 (2017).
[52] C. Zhou and H. Guo, Phys. Rev. B **95**, 035126 (2017).
[53] J. N. Zhuang and J. Wang, J. Appl. Phys. **144**, 063708 (2013).
[54] L. S. Levitov, in *Quantum Noise in Mesoscopic Physics*, edited by Yu. V. Nazarov, NATO Science Series, II, Mathematics, Physics and Chemistry Vol. 97 (Kluwer, Dordrecht, 2003).
[55] L. S. Levitov and G. B. Lesovik, Pis'ma Zh. Eksp. Teor. Fiz. **58**, 225 (1993) [Sov. Phys. JETP **58**, 230 (1993)].
[56] L. S. Levitov, H.-W. Lee, and G. B. Lesovik, J. Math. Phys. **37**, 4845 (1996).
[57] G. M. Tang and J. Wang, Phys. Rev. B **90**, 195422 (2014).
[58] B. Fu, L. Zhang, Y. D. Wei, and J. Wang, Phys. Rev. B **96**, 115410 (2017).
[59] D. S. Fisher and P. A. Lee, Phys. Rev. B **23**, 6851(R) (1981).
[60] M. Buttiker, Phys. Rev. B **46**, 12485 (1992).
[61] J. Wang and H. Guo, Phys. Rev. B **79**, 045119 (2009).
[62] S. Datta, *Electronic Transport in Mesoscopic Systems* (Cambridge University Press, New York, 1995), pp. 137–148.